

200936115A

平成 21 年度 厚生労働科学研究費補助金
難治性疾患克服研究事業

ペルオキシソーム病:副腎白ジストロフィーの生体試
料収集及び、臨床病型修飾因子についての研究

課題番号: H21-難治-一般-060

平成 21 年度 総括研究報告書

平成 22(2010)年 3 月

研究代表者 後藤 順

目 次

I. 総括研究報告

ペルオキシソーム病:副腎白質ジストロフィーの生体試料収集
及び、臨床病型修飾因子についての研究・・・・・・・・・・3

後藤 順

II. 研究成果の刊行に関する一覧表・・・・・・・・・・10

III.研究成果の刊行物・別冊・・・・・・・・・・12

I. 総括研究報告

厚生労働科学研究費補助金（難治性疾患克服研究事業）

総括研究報告書

ペルオキシシソーム病：副腎白ジストロフィーの生体試料収集及び、臨床病型修飾因子についての研究

研究代表者：後藤 順 東京大学医学部附属病院神経内科講師

研 究 要 旨

副腎白質ジストロフィーには、いくつかの臨床型があり、小児大脳型では、発症後広範な白質病変が進行する。近年、小児大脳型においては、発症初期に造血幹細胞移植によって、進行を抑えられる。しかしながら、診断が遅れがちであり、病型を決定している要因は不明である。様々な課題を解決するため、永続的な ALD 研究リソースの構築及び維持が必要である。副腎白質ジストロフィー（ALD）の生体試料及び臨床情報による研究リソース収集及びバンクへ（基盤研）の寄託を目的として、東京大学（成人例）と岐阜大学（小児例）を拠点とする研究リソース収集の基盤体制構築のための研究を行った。臨床病型修飾因子の解明に関して、副腎白質ジストロフィー原因遺伝子 *ABCD1* の同族遺伝子 *ABCD2*, *3*, *4* の 3 遺伝子との関連解析を行った。*ABCD4* と副腎脊髄ニューロパチーとの関連が示唆された ($p = 0.047$) が、例数が十分とは言えず、今後の検討が必要である。

研 究 組 織

研究者名	所属機関	職 名
後藤 順	東京大学医学部附属病院神経内科・臨床ゲノム診療部	講 師
辻 省次	東京大学医学部附属病院神経内科・臨床ゲノム診療部	教 授
市川弥生子	東京大学医学部附属病院神経内科・臨床ゲノム診療部	助 教
高橋 祐二	東京大学医学部附属病院神経内科・臨床ゲノム診療部	助 教
下澤 伸行	岐阜大学生命総合研究支援センターゲノム分野	教 授

研究協力者：松川 敬志 東京大学医学部附属病院神経内科

研究目的

ペルオキシソーム病は、細胞小器官のひとつであるペルオキシソームの機能や形成障害による遺伝性の先天性代謝異常症である。副腎白質ジストロフィーは、ペルオキシソーム病の一つで、その中では最も頻度の高い疾患である。副腎白質ジストロフィーは、X連鎖劣性遺伝形式をとり、Xq28に位置する*ABCD1*遺伝子の突然変異による疾患で、男子において発症する。いくつかの病型を呈し、小児大脳型、副腎脊髄ニューロパチー、副腎不全などの病型を呈する。近年、小児大脳型においては、発症初期に造血幹細胞移植を行なうことによって、進行を抑えられることが示され、小児大脳型副腎白質ジストロフィーの治療法として普及しつつある。さらに、より侵襲性の低い、薬物療法などの開発も期待される。

発症年齢、臨床病型、重症度などを規定する因子(ホスト因子、環境因子)は解明されておらず、*ABCD1*遺伝子変異の種類と、臨床病型には関連がないことも確認されている。本研究の目的は、臨床病型の修飾因子を明らかにするために、日本の副腎白質ジストロフィー症例の多くについて、臨床情報と生体試料(ゲノムDNA、リンパ芽球細胞株)を収集し、ゲノム関連解析を始めとするゲノム解析による検討と、臨床情報に基づく疫学研究を進めること、同時に、このような生体試料と臨床情報について、すべての研究者がアクセスして、独自の研究に基づき研究を進めることができるようにする研究リソース基盤を構築することである。

方法

A. 副腎白質ジストロフィーの生体試料収集

図1に示す、副腎白質ジストロフィー(ALD)の生体試料収集体制の構築のため、以下の検討を行った。

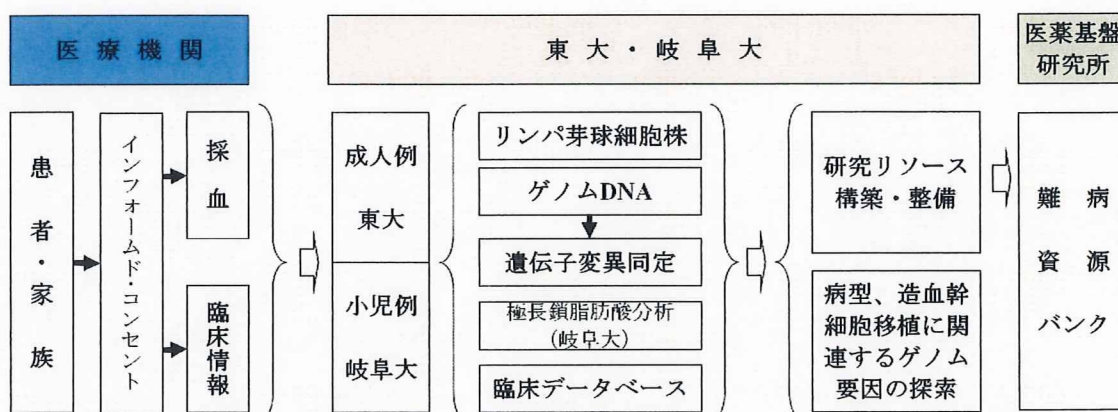


図1 副腎白質ジストロフィー(ALD)生体試料収集 成人例については東京大学、小児例については岐阜大学をそれぞれ、拠点として収集する。ゲノムDNA、リンパ芽球細胞株、臨床情報の収集を行う。*ABCD1*遺伝子変異の同定、極長鎖脂肪酸分析を行い、それらの結果を附帯した研究リソースを整備し、難病資源バンクに寄託する。

1. 過去収集試料の集計
2. インフォームド・コンセントの検討
3. 過去収集検体のバンクへの寄託
4. 収集すべき臨床情報項目

B. 臨床病型修飾因子についての検討

1. 対象: 副腎白質ジストロフィー 71 例 (大脳型 ALD 44 例、AMN 26 例)
対照 82 例
2. 上記対象者のゲノム DNA を定法に則り、末梢血白血球より抽出し、解析に用いた。
3. 副腎白質ジストロフィーの診断は、*ABCD1* の直接シーケンシング法によった。
4. 同一遺伝子ファミリーに分類される、*ABCD2*, *3*, *4* の 4 遺伝子について、エクソン領域を患者群において直接シーケンシング法によって解析した。同定された既知並びに新規 DNA 配列変異について、対照群について検討し、両群について比較検定した。
5. 「ヒトゲノム・遺伝子解析研究に関する倫理指針」、「疫学研究による倫理指針」、「臨床研究に関する倫理指針」を遵守し、研究倫理委員会の承認のもと行った。

結 果

A. 副腎白質ジストロフィーの生体試料収集

1. 過去に収集された副腎白質ジストロフィー生体試料の集計

東京大学、岐阜大学、新潟大学の 3 機関において過去に収集された生体試料として、ゲノム DNA の集計を表 1 にまとめた。一部、東京大学においてはリンパ芽球細胞株を、岐阜大学においては線維芽細胞を保存している。

表1 過去に収集された副腎白質ジストロフィーのゲノム DNA 試料

研 究 機 関	例 数
東 京 大 学	32 例
岐 阜 大 学	71 例 (58 家系)
新 潟 大 学	18 例
計	121 例

2. インフォームド・コンセントについて

共通の様式にて、難病資源バンク (基盤研) への寄託についての同意を盛り込んだインフォームド・コンセントとする。

3. 過去収集検体について

バンクへの寄託のコンセントのある検体については、研究倫理審査委員会での承認等必要な手続きの上、バンクへの寄託を進める。

(5) 遺伝子診断

III. 治 療

(1) 血液幹細胞移植

B. 臨床病型修飾因子についての検討

1. ABCD ファミリー遺伝子の一塩基多型 (SNPs)

ABCD2, *3*, *4* のエクソンを直接シーケンス法にて解析した。dbSNP に登録されている既知の一塩基多型 (SNPs) 以外に、*ABCD2* では 2 箇所、*ABCD3* では 3 箇所、*ABCD4* では 6 箇所の計 11 箇所の新規一塩基多型を同定した (図2)。

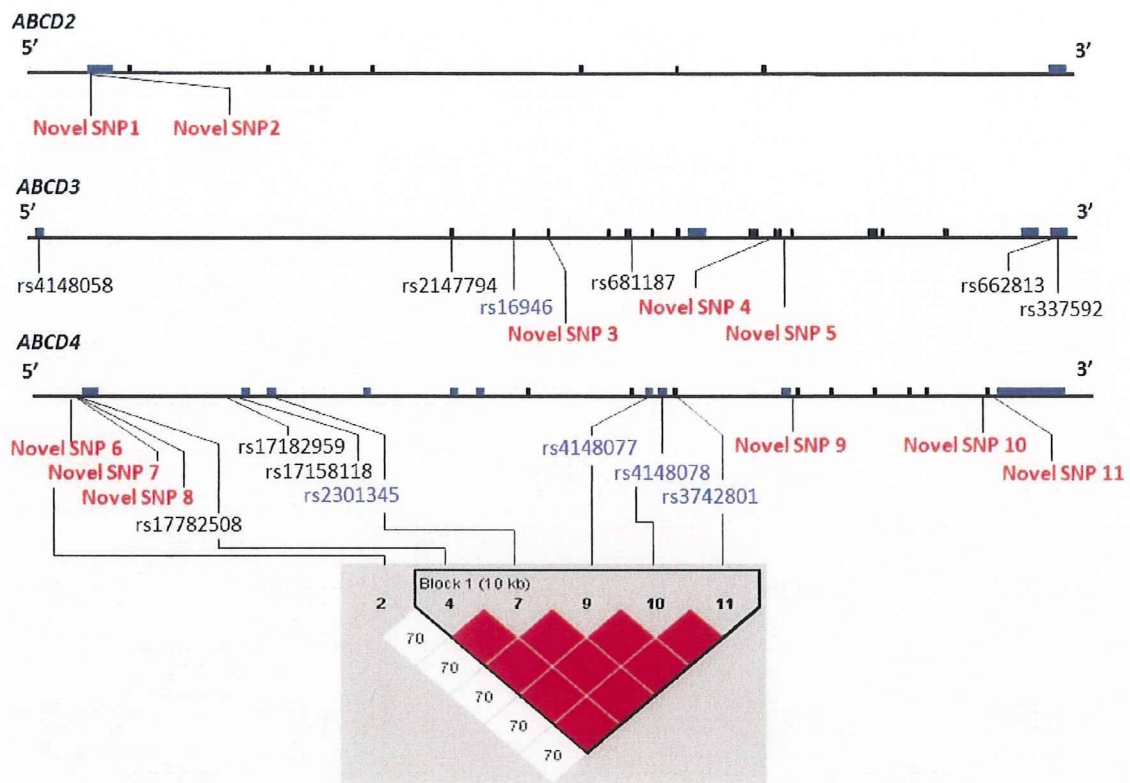


図2 *ABCD2*, *3*, *4* 遺伝子の一塩基多型 赤は、本研究で新たに同定した新規一塩基多型。Rs17782508, rs2301345, rs4148077, rs4148078, rs3742801 は完全連鎖不平衡。

2. 関連解析

ABCD2 の 2 箇所、*ABCD3* の 9 箇所、*ABCD4* の 13 箇所の一塩基多型について関連解析を行った。いずれの多型についても ALD 全体との関連は認めなかった。病型別の解析で、副腎脊髄ニューロパチー (AMN) と *ABCD4* の完全連鎖不平衡にある多型との間に、 $p = 0.0468$ と関連が示唆された (表2)。

表2 ABCD4 の rs17782508-rs2301345-rs4148077-rs4148078-rs3742801 と AMN との関連

SNPs	p 値		
	大脳型 対 AMN	大脳型 対 対照	AMN 対 対照
rs17782508	0.1921	0.5575	0.0468
rs2301345	0.1921	0.5575	0.0468
rs4148077	0.1921	0.5575	0.0468
rs4148078	0.1921	0.5575	0.0468
rs3742801	0.1921	0.5575	0.0468

考 察

副腎白質ジストロフィー (ALD) の生体試料 (主にゲノム DNA) は、これまでに国内の 3 研究機関 (東京大学、岐阜大学、新潟大学) で、計 121 例分が収集されていた。

臨床情報の収集項目を策定し、難病資源バンク (基盤研) への寄託を前提としたインフォームド・コンセントによる試料収集を進め、研究リソースを拡充することが重要である。希少疾患であることを考慮し、課題も多いが、過去に収集された試料も広く研究リソースとして利用可能とする条件・方法の検討も必要と考えられる。

臨床病型修飾因子の検討を目的として、ABCD ファミリー遺伝子との関連解析を行った。ABCD4 と AMN との関連が示唆されたが、小規模の解析であり、さらなる検討が必要である。

結 論

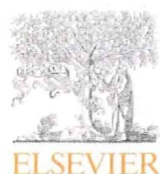
副腎白質ジストロフィー (ALD) の生体試料及び臨床情報による研究リソース収集及びバンクへの寄託体制の基盤構築が可能となった。

Ⅱ．研究成果の刊行に関する一覧

研究成果の刊行に関する一覧表

発表者氏名	論文タイトル名	発表雑誌名	巻数	ページ	出版年
Matsumoto H, Hanajima R, Terao Y, Hamada M, Yugeta A, Shirota Y, Yuasa K, Sato F, Matsukawa T, <u>Takahashi Y, Goto J,</u> <u>Tsuji S</u> , Ugawa Y	Efferent and afferent evoked potentials in patients with adrenomyeloneuropat hy.	Clin Neurol Neurosurg.	112	131-136	2010
Al-Dirbashi OY, Shaheen R, Al-Sayed M, Al-Dosari M, Makhseed N, Safieh LA, Santa T, Meyer BF, <u>Shimozawa N,</u> Alkuraya FS	Zellweger syndrome caused by PEX13 deficiency: Report of two novel mutations.	Am J Med Genet	149A	1219-1223	2009
<u>下澤 伸行</u>	先天代謝異常症 ペルオキシソーム病	小児内科	41	479-486	2009
<u>下澤 伸行</u>	日本人が発見に関わ った疾患遺伝子 ペ ルオキシソーム病	小児科	50	907-913	2009

Ⅲ. 研究成果の刊行物・別刷



Efferent and afferent evoked potentials in patients with adrenomyeloneuropathy

Hideyuki Matsumoto^{a,†}, Ritsuko Hanajima^a, Yasuo Terao^a, Masashi Hamada^a, Akihiro Yugeta^a,
Yuichiro Shirota^a, Kaoru Yuasa^a, Fumio Sato^a, Takashi Matsukawa^a, Yuji Takahashi^a,
Jun Goto^a, Shoji Tsuji^a, Yoshikazu Ugawa^b

^a Department of Neurology, Division of Neuroscience, Graduate School of Medicine, University of Tokyo, 7-3-1 Hongo, Bunkyo-ku, Tokyo 113-8655, Japan

^b Department of Neurology, School of Medicine, Fukushima Medical University, Japan

ARTICLE INFO

Article history:

Received 8 April 2009

Received in revised form 4 November 2009

Accepted 6 November 2009

Available online 5 December 2009

Keywords:

Magnetic stimulation
Evoked potential
Adrenoleukodystrophy
Adrenomyeloneuropathy
Axonopathy
Myelinopathy

ABSTRACT

Objective: This paper investigates efferent and afferent conductions of the central nervous system by various evoked potentials in patients with adrenomyeloneuropathy (AMN).

Patients and methods: Ten pure AMN patients without cerebral involvement were studied. Motor evoked potentials (MEPs), somatosensory evoked potentials (SEPs), auditory brainstem response (ABR), and pattern reversal full-field visual evoked potentials (VEPs) were recorded. For MEP recording, single-pulse or double-pulse magnetic brainstem stimulation (BST) was also performed.

Results: Abnormal MEP was observed in all ten patients, abnormal SEP in all ten, abnormal ABR in nine, and abnormal VEP in only one. Brainstem latency was measured in three of the seven patients with central motor conduction time (CMCT) prolongation. The cortical–brainstem conduction time was severely prolonged along the normal or mildly delayed brainstem–cervical conduction time in those three patients.

Conclusions: The pattern of normal VEP and abnormal MEP, SEP, ABR is a clinically useful electrophysiological feature for the diagnosis. BST techniques are helpful to detect, functionally, intracranial corticospinal tract involvement, probably demyelination, in pure AMN patients.

© 2009 Elsevier B.V. All rights reserved.

1. Introduction

X-linked adrenoleukodystrophy (ALD) is a peroxisomal disorder caused by mutation of the ABCD1 gene [1] whose biochemical abnormality is characterized by the accumulation of very long chain saturated fatty acids (VLCFA) [2–5]. The highly varied phenotype of X-linked ALD is classified into subtypes such as childhood cerebral ALD, adolescent cerebral ALD, adrenomyeloneuropathy (AMN), adult cerebral ALD, olivo-ponto-cerebellar ALD and Addison's disease-only ALD [6–8]. No correlation exists between phenotypes and genotypes [9]. The central nervous system pathology comprises two apparently disparate types of cerebral form (cerebral ALD) and AMN. The cerebral ALD is characterized by a severe inflammatory demyelinating lesion in the cerebrum (myelinopathy) [10]. The AMN is characterized by distal axonopathy: degeneration of spinal tracts distributed in a 'dying-back' pattern [11]. These two major forms of the disease differ fundamentally with respect to their prognoses. Although rapidly progressive cerebral ALD engenders total disability during the first decade, some patients with AMN survive to the eighth decade [6]. However, about half of the AMN patients clinically develop cerebral involvement within 10 years after onset

[7,8]. The patients without cerebral involvement are referred to as "pure" AMN, whereas the patients with cerebral involvement are referred to as "cerebral" AMN. The magnetic resonance image (MRI) in pure AMN is often normal but may show changes up to the internal capsule [12,13], and the corticospinal tract lesions in pure AMN are considered to be axonal pathology [12,14,15]. On the other hand, the pathological mechanism in cerebral AMN is proposed to be the cerebral demyelination in addition to the distal axonopathy [12]. Therefore, the assessment of brain function using neurophysiological methods is very important in considering prognosis and possible treatment in AMN patients [6].

Central efferent function is physiologically examined using motor evoked potential (MEP). In fact, MEP studies have revealed frequent abnormal central motor conduction in AMN patients [16–18]. The central motor conduction time (CMCT) mainly reflects the overall function of the motor tract of the central nervous system. However, it does not indicate the level of motor tract involvement: whether it is intracranial, extracranial, or both. We previously developed methods to activate the descending motor tracts at the level of the pyramidal decussation (foramen magnum) using electrical stimulation [19] and magnetic stimulation [20]. The methods [brainstem stimulation (BST)] have been shown to be clinically useful for localizing corticospinal tract lesions in patients with various neurological disorders [21–25]. For this investigation, we applied this stimulation along with cortical and spinal stimulations to show

[†] Corresponding author. Tel.: +81 3 5800 8672; fax: +81 3 5800 6548.
E-mail address: hideyukimatsumoto@mail.goo.ne.jp (H. Matsumoto).

Table 1
Background of patients.

Case	Age	ABCD1 mutation	Disease duration (years)	Main symptom(s)	Brain MRI	Loes score	Spinal MRI
1	32	Missense (H667N)	1	Spastic gait, pigmentation	Normal	0	Normal
2	44	Nonsense (W595X)	1	Spastic gait, sensory disturbance (leg)	Normal	0	Atrophy
3	61	N.E.	4	Spastic gait, muscular weakness (leg), sensory disturbance (leg)	Normal	0	Normal
4	30	Missense (S290W)	5	Spastic gait, sensory disturbance (leg), dysuria, dyschezia, impotence	P, V	2.5	Normal
5	31	Missense (F540S)	5	Spastic gait	V	0.5	Normal
6	24	Missense (A616D)	6	Spastic gait, sensory disturbance (leg), dysuria, impotence	Normal	0	Normal
7	31	Frameshift (Y281)	8	Spastic gait, sensory disturbance (leg), dyschezia	C	0.5	Normal
8	33	Missense (G277R)	8	Spastic gait, dysuria, dyschezia impotence	P	2	Atrophy
9	58	N.E.	18	Spastic gait, dysuria	Normal	0	Atrophy
10	58	N.E.	19	Spastic gait, impotence	Normal	0	Normal

MRI: magnetic resonance image, P: pyramidal system, V: visual pathway, C: cerebellum, N.E.: not examined.

which part of the descending tract was affected. We also adopted a recently reported powerful stimulation method to evoke clear MEPs in patients without any MEPs to single-pulse BST: double-pulse magnetic BST [26].

The central afferent functions are usually studied with various evoked potentials such as somatosensory evoked potential (SEP), auditory brainstem response (ABR), and visual evoked potential (VEP). These three evoked potentials also have shown afferent system conduction abnormalities in AMN patients [16,17,27–32].

The aim of this study is to investigate efferent and afferent conductions of the central nervous system in pure AMN patients using the four types of evoked potentials including magnetic BST. Some results of MEPs in this study were described in a previous report [26].

2. Methods

2.1. Patients

We studied ten male patients with AMN. Based on the course of the disease and clinical symptoms, they were diagnosed as AMN. Plasma VLCFA was abnormally increased in all of them. The ABCD1 gene mutation was analyzed in seven patients (cases 1, 2, 4–8) after receiving their informed consent [33,34]. Their patient characteristics and clinical features are presented in Table 1. Their ages were 24–61 years (mean \pm SD, 40.2 ± 13.9 years). Their body heights were 165–175 cm (169.1 ± 3.2 cm). The durations of illness at the time of our experiment were 1–19 years (7.5 ± 6.3 years). All patients presented with spastic paraplegia with positive Babinski signs. Five patients presented with diminished superficial and deep sensation in the lower extremities (cases 2–4, 6, and 7). On the other hand, all patients presented no symptoms of motor and sensory systems in the upper extremities. They all also had no auditory and visual complaints. Brain and spinal MRIs were also taken. The lesions observed on brain MRI were described according to a previous paper [35]. Because all patients had no clinical or radiological cerebral involvement, all of them were classified into pure AMN [12,13]. Both MEP and SEP were recorded on the more affected side of motor symptom; ABR and VEP were recorded on both sides. We compared the latencies of these evoked potentials with the normal values in our institution.

Informed consent to participate in this study was obtained from all patients. The protocol was approved by the Ethics Committee of the University of Tokyo. It was conducted in accordance with the ethical standards of the Declaration of Helsinki.

2.2. MEP recording

Patients were seated comfortably on a reclining chair. MEPs were recorded from the first dorsal interosseous (FDI) and tibialis

anterior (TA) muscles with pairs of Ag/AgCl surface cup electrodes placed in a belly tendon montage. Signals were fed to an amplifier (Biotop; GE Marquette Medical System, Japan) with filters set at 100 Hz and 3 kHz; the signals were recorded using software (TMS bistim tester; Medical Try System, Japan) for later off-line analyses.

Magnetic stimulation was conducted using a monophasic stimulator (Magstim 200; The Magstim Co. Ltd., UK) for transcranial magnetic stimulation (TMS), magnetic spinal motor root stimulation, and single-pulse BST. Double-pulse BST was given by connecting the two magnetic stimulators linked with a Bistim module (The Magstim Co. Ltd., UK).

For both muscles, CMCT was measured in each patient. For FDI, the onset latency of MEP elicited by TMS over the contralateral hand motor area using a round coil (10 cm diameter; The Magstim Co. Ltd., UK) was measured in the active condition (cortical latency). Induced current flowed in the posterior to the anterior direction over the hand motor area [36,37]. For TA, cortical latency was measured placing a double-cone-coil (The Magstim Co. Ltd., UK) [38] over the Cz (international 10–20 system), with induced current flowing mediolaterally over the leg motor area [39]. The onset latency of MEP to magnetic spinal motor root stimulation was also measured by activating cervical and lumbar spinal nerves with a round coil (10 cm diameter) placed over the spinal enlargement (spinal latency) [40,41]. The CMCT was calculated by subtracting the spinal latency from the cortical latency [37].

For FDI, single-pulse BST was also performed in active and relaxed conditions [20]. For BST, a double-cone-coil was placed with the center of the junction region over the union. The coil current flowed downward at the junction of the coil so that the maximal current induced in the head flowed upward because this current direction has the lowest threshold for evoking MEPs [23]. The onset latency of MEP to single-pulse BST was measured (brainstem latency). When a single-pulse BST with maximal stimulator output was insufficient to evoke any MEP, double-pulse BST at an interstimulus interval of 2 ms was tried in a relaxed condition [26]. The stimulus intensities of double-pulse BST were set at the maximal stimulator output. The onset latency of MEP to double-pulse BST was measured from the time of the second pulse, which was identical to that of single-pulse BST (brainstem latency) [26]. The cortical–brainstem and brainstem–cervical conduction times were obtained, respectively, by subtracting the brainstem latency from the cortical latency and the spinal latency from the brainstem latency.

2.3. SEP recording

For this study, the SEPs were elicited after electrical stimulation (a constant current square wave pulse with duration of 0.2 ms) of the median nerve at the wrist or posterior tibial nerve at the ankle, as described in previous reports [16]. For recording N13 and

Table 2
Results of one efferent evoked potential.

Case	Side	MEP (FDI) cervical	CMCT	Cortical–BST	BST–cervical	MEP (TA) lumbar	CMCT (ms)
1	Rt	13.9	7.2	2.9	4.3	14.3	21.0 †
2	Rt	12.5	8.6 †	N.E.		12.1	23.3 †
3	Lt	17.3 †	6.0	1.7	4.3	17.1 †	19.5 †
4	Rt	12.4	13.0 †	7.8 †	5.2 †	12.8	30.1 †
5	Lt	13.5	15.4 †	N.D.		15.1	N.D.
6	Rt	14.0	12.8 †	N.D.		11.8	N.D.
7	Lt	12.0	11.3 †	N.D.		11.6	N.D.
8	Rt	14.3	8.6 †	5.1 †	3.5	14.8	26.8 †
9	Rt	14.7	10.3 †	6.2 †	4.1	17.0 †	18.7 †
10	Rt	12.8	7.0	3.2	3.8	15.6	21.3 †
Normal values (upper limit, +2.5 SD)		15.1	8.0	4.1	5.0	16.7	17.8

MEP: motor evoked potential, FDI: first dorsal interosseous, TA: tibialis anterior, CMCT: central motor conduction time, cortical–BST: cortical–brainstem conduction time, BST–cervical: brainstem–cervical conduction time, †: prolonged latency, N.E.: not examined, N.D.: not detected, bold type: abnormal findings.

N20 potentials elicited by median nerve stimulation, the electrodes were placed at two locations: the spinous process of C6 and C3' or C4' (2 cm posterior to the C3 or C4, the international 10–20 system), with Fz reference. For recording N21 and P38 potentials evoked by tibial nerve stimulation, the recording electrodes were placed at two locations: the spinous process of L1 with contralateral iliac crest reference, and Cz' (2 cm posterior to the Cz) with Fz reference. For the median nerve SEP, the peak latency of N13 and the inter-peak latency of N13–N20 were measured, and for the tibial nerve SEP, the N21 peak latency and the N21–P38 inter-peak latency were measured. The inter-peak latencies, N13–N20 and N21–P38, are conventionally called the cortical sensory conduction time (CSCT) whereas the peak latencies, N13 and N21, are called the peripheral conduction time [16,42].

2.4. ABR recording

The ABR was recorded as reported in our previous report [43]. The recording electrode was placed over the vertex (Cz) and the reference electrode on the unilateral earlobe, and the ground electrode was over the Fz. An 80 dB (equivalent sound pressure level, 100 μ s duration, alternating) click sound was given to the unilat-

eral ear on the reference side at a rate of 5 Hz with a headphone; both sides were examined separately. The peak latencies of I and V waves were measured, and the inter-peak latency between I and V waves was calculated. The neural generator of I wave in humans is considered as the acoustic nerve; that of the V wave is the auditory interneurons at the level of the inferior colliculus [44]. Therefore, the inter-peak latency of I–V waves is mainly expected to reflect the central auditory conduction.

2.5. VEP recording

Monocular pattern reversal full-field VEP was recorded. A black-and-white checkerboard pattern placed 127 cm in front of the subjects was reversed at 1 Hz. The total stimulus visual angle and each check subtended angle of 16×12 degrees and 60 min, respectively. One eye was covered with an eye patch; both eyes were examined alternately. The three recording electrodes were placed in the mid-occipital (MO), in midline 5 cm above theinion, the left-occipital (LO), in left 5 cm of MO, and the right-occipital (RO), in right 5 cm of MO. A mid-frontal (MF) electrode placed 12 cm above the nasion as the references. The latency of the major positive peak of the VEP (P 100) was determined.

Table 3
Results of three afferent evoked potentials.

Case	Side	SEP (median)		SEP (tibial)		Side	ABR		VEP, P 100 (ms)
		N13	N13–N20	N21	N21–P38		I	I–V	
1	Rt	14.3	7.1 †	23.4	18.2	Lt	1.43	5.58 †	109.0
						Rt	1.41	5.29 †	109.0
2	Rt	13.6	8.9 †	21.6	23.6 †	Lt	1.48	5.72 †	106.5
						Rt	1.43	5.75 †	99.3
3	Lt	16.8 †	6.7	29.8 †	19.0	Lt	1.50	5.14 †	110.0
						Rt	1.45	4.67 †	109.8
4	Rt	13.3	8.0 †	20.9	38.9 †	Lt	1.52	5.48 †	107.1
						Rt	1.70	5.16 †	103.2
5	Lt	15.5 †	7.5 †	24.1	31.8 †	Lt	1.52	5.49 †	105.3
						Rt	1.89	4.63 †	106.8
6	Rt	15.1	9.3 †	20.5	N.D.	Lt	1.54	5.08 †	149.4 †
						Rt	1.49	4.99 †	146.6 †
7	Lt	14.3	7.0 †	21.0	29.8 †	Lt	1.57	5.06 †	97.0
						Rt	1.49	4.83 †	96.0
8	Rt	14.8	7.2 †	24.6 †	25.0 †	Lt	1.86	5.39 †	97.5
						Rt	1.57	5.41 †	99.3
9	Rt	16.2 †	6.4	26.3 †	19.8	Lt	1.33	5.22 †	113.7
						Rt	1.38	4.81 †	113.1
10	Rt	N.E.		20.3	33.7†	Lt	1.77	4.25 †	102.3
						Rt	1.78	4.10	94.5
Normal values (upper limit, +2.5 SD)		15.3	6.8	24.4	20.5		1.92	4.57	114.1

SEP: sensory evoked potential, VEP: visual evoked potential, ABR: auditory brainstem response, †: prolonged latency, N.E.: not examined, N.D.: not detected, bold type: abnormal findings.

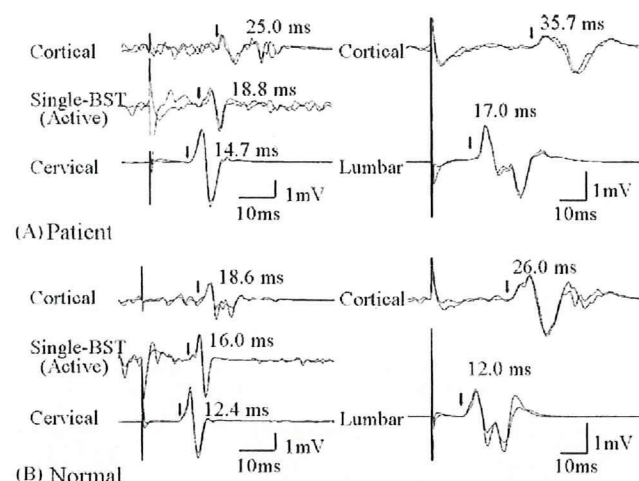


Fig. 1. MEP study in case 9. (A) MEP in a representative patient (case 9). Left figure shows MEPs recorded from FDI. CMCT is prolonged (10.3 ms, upper limit of normal values 8.0 ms). Only the cortical-brainstem conduction time is prolonged (6.2 ms, upper limit 4.1 ms), suggesting corticospinal tract involvement at the intracranial level. Right figure shows MEPs recorded from TA. CMCT is 18.7 ms (upper limit 17.8 ms) and spinal latency is 17.0 ms (upper limit 16.7 ms), indicating both central and peripheral motor conduction delays. (B) MEP in a normal subject.

3. Results

The results of one efferent evoked potential and three afferent evoked potentials are presented in Tables 2 and 3. The P 100 latency of VEP was measured in the montage of MO–MF where the maximal amplitude was obtained in all ten patients.

Fig. 1 displays the waveforms of MEP in case 9 as an illustration. The CMCTs and spinal latencies for FDI and TA were measured in all AMN patients. For FDI, the CMCT was prolonged in seven patients (cases 2, 4, 5, 6, 7, 8, and 9). The spinal latency for FDI was prolonged in one patient (case 3). For TA, the CMCT was prolonged in seven patients or MEPs were not detected in the other three patients (cases 5, 6, and 7). The spinal latency for TA was prolonged in two patients (cases 3 and 9). Single-pulse or double-pulse BST was performed in nine of ten patients [one patient (case 2) declined to participate in the BST experiments]. Single-pulse BST elicited MEPs in five patients (cases 1, 3, 8, 9, and 10). Double-pulse BST was given to the other five patients, and evoked MEPs in one patient (case 4). Consequently, brainstem latency was measured in six patients (cases 1, 3, 4, 8, 9, and 10). In two patients (cases 8 and 9), the cortical–brainstem conduction time was prolonged (case 8: 5.1 ms, case 9: 6.2 ms, upper limit: 4.1 ms) but the brainstem–cervical conduction time was normal (case 8: 3.5 ms, case 9: 4.1 ms, upper limit: 5.0 ms). In one patient (case 4), both the cortical–brainstem and brainstem–cervical conduction times were prolonged (7.8 ms and 5.2 ms, respectively) but prolongation of the former conduction time was predominant. In three patients (cases 1, 3 and 10) with normal CMCT, both conduction times were normal.

Fig. 2 displays the representative waveforms of SEP (case 7). In the median nerve SEP, the CSCT was prolonged in seven of nine patients studied (cases 1, 2, 4, 5, 6, 7, and 8). Median nerve SEP was not examined in one patient (case 10). The peripheral conduction was prolonged in three of them (cases 3, 5, and 9). Regarding the tibial nerve SEP, the CSCT was prolonged or SEPs were not evoked in seven patients (cases 2, 4, 5, 6, 7, 8, and 10); the peripheral conduction time was prolonged in three patients (cases 3, 8, and 9). Fig. 3 displays the waveforms of ABR and VEP in case 6 as a representative of cases. The inter-peak latency of I–V waves of ABR was prolonged in nine patients and normal in one patient (case 10). The

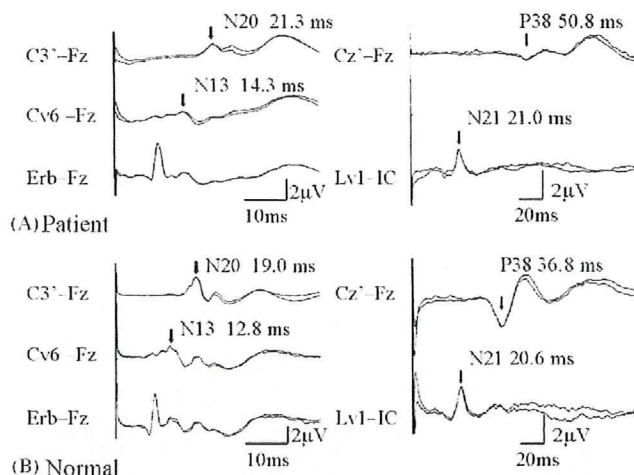


Fig. 2. SEP study in case 7. (A) SEP in a representative patient (case 7). Left figure shows the median nerve SEP. The bottom traces show the responses at the ipsilateral Erb's point to record peripheral nerve volley. N13–N20 latency is 7.0 ms (upper limit of normal values 6.8 ms) and N13 latency is 14.3 ms (upper limit 15.3 ms), indicating only CSCT prolongation. Right figure shows the tibial nerve SEP. CSCT (N21–P38 latency) is prolonged (29.8 ms, upper limit 20.5 ms). (B) SEP in a normal subject.

I wave latency was within normal limit in all patients. The P 100 latency was prolonged in only one of ten patients (case 6).

Brain MRI revealed abnormalities in four patients (cases 4, 5, 7, and 8) and no abnormalities in the other six patients. The pyramidal tract lesions (cases 4 and 8: Loes score 2), questionable optic radiation lesions (cases 4 and 5: Loes score 0.5) and unilateral cerebellum lesions (case 7: Loes score 0.5) were observed. Cerebral white matter was preserved in all patients. Spinal MRI showed atrophy of the spinal cord in three patients (cases 2, 8, and 9) and no abnormalities in the other patients.

MEP and SEP abnormalities were observed in all patients, although only four patients (cases 2, 4, 8, and 9) exhibited MRI abnormalities in the motor and sensory pathways (pyramidal tract lesions or spinal cord atrophy). ABR abnormalities were observed in nine patients except one patient (case 10), although no auditory

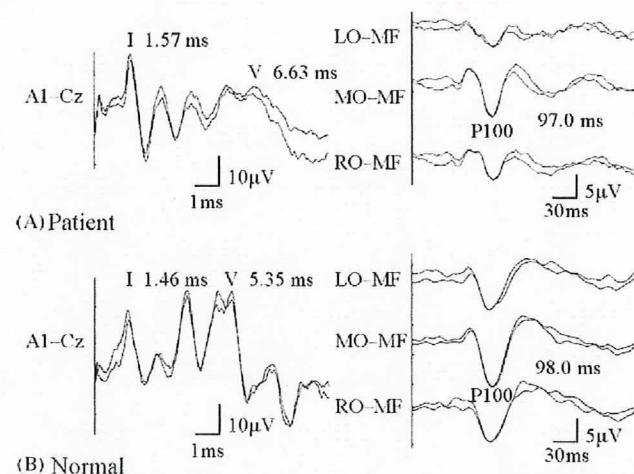


Fig. 3. ABR and VEP studies in case 7. (A) ABR and VEP in a representative patient (case 7). Left figure shows ABR waveforms in A1–Cz montage evoked by left sound stimulation. I wave latency is normal (1.57 ms, upper limit of normal values 1.92 ms), whereas I–V latency is prolonged (5.06 ms, upper limit 4.57 ms), suggesting the central auditory conduction delay. Right figure shows the VEP waveforms evoked by left monocular full-field stimulation. The maximal amplitude is obtained in the MO–MF montage. The P 100 latency is within normal limit (97.0 ms, upper limit 114.1 ms). (B) ABR and VEP in a normal subject.

pathway lesions were found in any of the ten patients. VEP abnormalities were seen in only one patient (case 6) whose brain MRI showed no visual pathway lesions.

Analyses of these patients yielded important physiological results. Every evoked potential revealed an abnormal conduction, even though MRIs showed normal findings. Regarding central efferent conduction, the cortical–brainstem conduction time was much more prolonged than the brainstem–cervical conduction time (cases 4, 8, and 9).

4. Discussion

This study revealed several physiological features in pure AMN patients. Although motor and sensory functions in the upper extremities were normal in all patients, both MEP and SEP in the upper extremities exhibited abnormal findings in eight patients. Similarly, despite normal auditory and visual functions, ABR and VEP could depict abnormalities, in nine patients and one patient, respectively. Thus, evoked potentials can detect subclinical lesions in the central nervous systems [45]. In addition, evoked potentials often revealed functional abnormalities of efferent and afferent conduction, even before any changes in MRI were evident, which is compatible with results described in the relevant literature [16,28,29,31].

The frequencies with which these evoked potentials detected abnormal conduction differed among these methods: MEP, SEP, and ABR were, respectively, abnormal in ten, ten, and nine of ten patients. In contrast, VEP was abnormal in only one out of ten patients. Therefore, MEP, SEP, and ABR abnormalities were more often observed than those of VEP. In fact, MEP, SEP, and ABR abnormalities are frequent findings in AMN patients [16,17,27,28,30–32]. In contrast, the incidence of pattern reversal full-field VEP abnormalities is not high in AMN patients (only 15 out of 59 AMN patients, 25.4%) [29]. Therefore, our studies verified the assumption from the prior studies, and we can regard normal pattern-reversal full-field VEP and abnormal MEP, SEP, and ABR patterns as an important neurophysiological feature that is frequently observed in this disorder.

In central efferent conduction, BST studies revealed severely delayed cortical–brainstem conduction time along the normal or mildly delayed brainstem–cervical conduction time in three pure AMN patients. Single-pulse BST failed to evoke MEPs in four out of nine patients. Single-pulse BST usually can evoke MEPs in FDI in healthy volunteers [20,26]. Therefore, the result implies that the threshold for BST was abnormally high in this disorder. Double-pulse BST was useful to detect these conduction delays, even in patients with no MEPs to single-pulse BST. Here we discuss the clinical significances of a newly discovered physiological feature in pure AMN: severely delayed cortical–brainstem conduction time.

Several mechanisms of severely delayed cortical–brainstem conduction time are considered to contribute to the prolongation of these conduction times [21,46]: (i) slowing of conduction in corticospinal tract fibers of large diameter (e.g. demyelinating disease), (ii) reduction in size (and number) of excitatory postsynaptic potentials generated by cortical or brainstem stimulation (e.g. amyotrophic lateral sclerosis), and (iii) reduction in the number of descending volleys induced by cortical stimulation caused by damage of cortical interneurons (e.g. cerebrovascular disease). Whatever the mechanism, the prolongation of the cortical–brainstem and brainstem–cervical conduction time can be taken to suggest that the corticospinal tract was affected, respectively, at the intracranial and extracranial levels [21].

Based on these discussions, we conclude that BST techniques are helpful to detect, functionally, intracranial corticospinal tract involvement in pure AMN patients. However, the prominent intracranial motor tract involvement in pure AMN patients cannot

be explained solely by the main pathological mechanism, i.e. predominant spinal cord lesions (distal axonopathy). Consequently, we consider that the physiological results in the BST study probably indicate demyelination in the intracranial corticospinal tract for the following two reasons. About half of the pure AMN patients clinically develop the phenotype of cerebral AMN such as cerebral ALD [7,8]. In addition, autopsy studies of AMN patients have also shown mild intracranial demyelination [11]. Therefore, in other words, BST techniques might detect intracranial demyelination in pure AMN. For the proof of this possibility, more studies using various methodologies must be necessary.

5. Conclusion

The pattern of normal pattern reversal full-field VEP and abnormal MEP, SEP, and ABR is a clinically important neurophysiological feature for the diagnosis. The combination techniques of single-pulse and double-pulse BST are helpful to detect, functionally, intracranial corticospinal tract involvement, probably demyelination, in pure AMN patients.

Acknowledgments

This work was supported by the Daiwa Anglo-Japanese Foundation; by Research Project Grants-in-aid for Scientific Research No. 17590865 (RH), No. 18590928 (YT) from the Ministry of Education, Culture, Sports, Science and Technology of Japan; by grants for the Research Committee on rTMS Treatment of Movement Disorders from the Ministry of Health and Welfare of Japan (17231401); by the Research Committee on Dystonia of the Ministry of Health and Welfare of Japan; by a grant from the Committee of the study of Human Exposure to EMF from the Ministry of Public Management, Home Affairs, Post and Telecommunications; and by grants from the Life Science Foundation of Japan.

References

- [1] Mosser J, Douar AM, Sarde CO, Kioschis P, Feil R, Moser H, et al. Putative X-linked adrenoleukodystrophy gene shares unexpected homology with ABC transporters. *Nature* 1993;361:726–30.
- [2] Igarashi M, Schaumburg HH, Powers J, Kishimoto Y, Kolodny E, Suzuki K. Fatty acid abnormality in adrenoleukodystrophy. *J Neurochem* 1976;26(4):851–60.
- [3] Tsuji S, Suzuki M, Ariga T, Sekine M, Kuriyama M, Miyatake T. Abnormality of long-chain fatty acids in erythrocyte membrane sphingomyelin from patients with adrenoleukodystrophy. *J Neurochem* 1981;36:1046–9.
- [4] Moser HW, Moser AB, Frayer KK, Chen W, Schulman JD, O'Neill BP, et al. Adrenoleukodystrophy: increased plasma content of saturated very long chain fatty acids. *Neurology* 1981;31:1241–9.
- [5] Tsuji S, Sano-Kawamura T, Ariga T, Miyatake T. Metabolism of [17,18-3H2] hexacosanoic acid and [15,16-3H2] lignoceric acid in cultured skin fibroblasts from patients with adrenoleukodystrophy (ALD) and adrenomyeloneuropathy (AMN). *J Neurol Sci* 1985;71:359–67.
- [6] Moser HW. Adrenoleukodystrophy: phenotype, genetics, pathogenesis and therapy. *Brain* 1997;120:1485–508.
- [7] Takemoto Y, Suzuki Y, Tamakoshi A, Onodera O, Tsuji S, Hashimoto T, et al. Epidemiology of X-linked adrenoleukodystrophy in Japan. *J Hum Genet* 2002;47:590–3.
- [8] Suzuki Y, Takemoto Y, Shimozawa N, Imanaka T, Kato S, Furuya H, et al. Natural history of X-linked adrenoleukodystrophy in Japan. *Brain Dev* 2005;27:353–7.
- [9] Takano H, Koike R, Onodera O, Sasaki R, Tsuji S. Mutational analysis and genotype–phenotype correlation of 29 unrelated Japanese patients with X-linked adrenoleukodystrophy. *Arch Neurol* 1999;56:295–300.
- [10] Powers JM, Liu Y, Moser AB, Moser HW. The inflammatory myelinopathy of adrenoleukodystrophy: cells, effector molecules, and pathogenetic implications. *J Neuropathol Exp Neurol* 1992;51:630–43.
- [11] Schaumburg HH, Powers JM, Raine CS, Spencer PS, Griffin JW, Prineas JW, et al. Adrenomyeloneuropathy: a probable variant of adrenoleukodystrophy. II. General pathologic, neuropathologic, and biochemical aspects. *Neurology* 1977;27:1114–9.
- [12] Dubey P, Fatemi A, Huang H, Nagae-Poetscher L, Wakana S, Barker PB, et al. Diffusion tensor-based imaging reveals occult abnormalities in adrenomyeloneuropathy. *Ann Neurol* 2005;58:758–66.
- [13] Dubey P, Fatemi A, Barker PB, Degaonkar M, Troeger M, Zackowski K, et al. Spectroscopic evidence of cerebral axonopathy in patients with “pure” adrenomyeloneuropathy. *Neurology* 2005;64:304–10.

- [14] Loes DJ, Fatemi A, Melhem ER, Gupta N, Bezman L, Moser HW, et al. Analysis of MRI patterns aids prediction of progression in X-linked adrenoleukodystrophy. *Neurology* 2003;61:369–74.
- [15] Kumar AJ, Köhler W, Kruse B, Naidu S, Bergin A, Edwin D, et al. MR findings in adult-onset adrenoleukodystrophy. *Am J Neuroradiol* 1995;16:1227–37.
- [16] Ugawa Y, Kohara N, Shimpō T, Mannen T. Central motor and sensory conduction in adrenoleukomyeloneuropathy, cerebrotendinous xanthomatosis, HTLV-1-associated myelopathy and tabes dorsalis. *J Neurol Neurosurg Psychiatry* 1988;51:1069–74.
- [17] Restuccia D, Di Lazzaro V, Valeriani M, Oliviero A, Le Pera D, Barba C, et al. Abnormalities of somatosensory and motor evoked potentials in adrenomyeloneuropathy: comparison with magnetic resonance imaging and clinical findings. *Muscle Nerve* 1997;20:1249–57.
- [18] Restuccia D, Di Lazzaro V, Valeriani M, Oliviero A, Le Pera D, Barba C, et al. Neurophysiologic follow-up of long-term dietary treatment in adult-onset adrenoleukodystrophy. *Neurology* 1999;52:810–6.
- [19] Ugawa Y, Rothwell JC, Day BL, Thompson PD, Marsden CD. Percutaneous electrical stimulation of corticospinal pathways at the level of the pyramidal decussation in humans. *Ann Neurol* 1991;29:418–27.
- [20] Ugawa Y, Uesaka Y, Terao Y, Hanajima R, Kanazawa I. Magnetic stimulation of corticospinal pathways at the foramen magnum level in humans. *Ann Neurol* 1994;36:618–24.
- [21] Ugawa Y, Genba K, Mannen T, Kanazawa I. Stimulation of corticospinal pathways at the level of the pyramidal decussation in neurological disorders. *Brain* 1992;115:1947–61.
- [22] Ugawa Y, Genba-Shimizu K, Kanazawa I. Electrical stimulation of the human descending motor tracts at several levels. *Can J Neurol Sci* 1995;22:36–42.
- [23] Ugawa Y, Uesaka Y, Terao Y, Suzuki M, Sakai K, Hanajima R, et al. Clinical utility of magnetic corticospinal tract stimulation at the foramen magnum level. *Electroencephalogr Clin Neurophysiol* 1996;101:247–54.
- [24] Ugawa Y. Stimulation at the foramen magnum level. *Electroencephalogr Clin Neurophysiol* 1999;51:S65–75.
- [25] Ugawa Y. Stimulation at the foramen magnum level as a tool to separate cortical from spinal cord excitability changes. *Adv Clin Neurophysiol (Suppl Clin Neurophysiol)* 2002;54:216–22.
- [26] Matsumoto H, Hanajima R, Hamada M, Terao Y, Yugeta A, Inomata-Terada S, et al. Double-pulse magnetic brainstem stimulation: mimicking successive descending volleys. *J Neurophysiol* 2008;100:3437–44.
- [27] Tobimatsu S, Fukui R, Kato M, Kobayashi T, Kuroiwa Y. Multimodality evoked potentials in patients and carriers with adrenoleukodystrophy and adrenomyeloneuropathy. *Electroencephalogr Clin Neurophysiol* 1985;62:18–24.
- [28] Aubourg P, Adamsbaum C, Lavallard-Rousseau MC, Lemaitre A, Boureau F, Mayer M, et al. Brain MRI and electrophysiologic abnormalities in preclinical and clinical adrenomyeloneuropathy. *Neurology* 1992;42:85–91.
- [29] Kaplan PW, Kruse B, Tusa RJ, Shankroff J, Rignani J, Moser HW. Visual system abnormalities in adrenomyeloneuropathy. *Ann Neurol* 1995;37:550–2.
- [30] Kaplan PW, Tusa RJ, Rignani J, Moser HW. Somatosensory evoked potentials in adrenomyeloneuropathy. *Neurology* 1997;48:1662–7.
- [31] van Geel BM, Assies J, Haverkort EB, Koelman JH, Verbeeten Jr B, Wanders RJ, et al. Progression of abnormalities in adrenomyeloneuropathy and neurologically asymptomatic X-linked adrenoleukodystrophy despite treatment with "Lorenzo's oil". *J Neurol Neurosurg Psychiatry* 1999;67:290–9.
- [32] Pillion JP, Kharkar S, Mahmood A, Moser H, Shimizu H. Auditory brainstem response findings and peripheral auditory sensitivity in adrenoleukodystrophy. *J Neurol Sci* 2006;247:130–7.
- [33] Takano H, Koike R, Onodera O, Tsuji S. Mutational analysis of X-linked adrenoleukodystrophy gene. *Cell Biochem Biophys* 2000;32:177–85.
- [34] Takahashi Y, Seki N, Ishiura H, Mitsui J, Matsukawa T, Kishino A, et al. Development of a high-throughput microarray-based resequencing system for neurological disorders and its application to molecular genetics of amyotrophic lateral sclerosis. *Arch Neurol* 2008;65:1326–32.
- [35] Loes DJ, Hite S, Moser H, Stillman AE, Shapiro E, Lockman L, et al. Adrenoleukodystrophy: a scoring method for brain MR observations. *Am J Neuroradiol* 1994;15:1761–6.
- [36] Barker AT, Jalinous R, Freeston IL. Non-invasive stimulation of human motor cortex. *Lancet* 1985;1:1106–7.
- [37] Rossini PM, Barker AT, Berardelli A, Caramia MD, Caruso G, Dimitrijević MR, et al. Non-invasive electrical and magnetic stimulation of the brain, spinal cord and roots: basic principles and procedures for routine clinical application. Report of an IFCN committee. *Electroencephalogr Clin Neurophysiol* 1994;91:79–92.
- [38] Terao Y, Ugawa Y, Sakai K, Uesaka Y, Kohara N, Kanazawa I. Transcranial stimulation of the leg area of the motor cortex in humans. *Acta Neurol Scand* 1994;89:378–83.
- [39] Terao Y, Ugawa Y, Hanajima R, Machii K, Furubayashi T, Mochizuki H, et al. Predominant activation of I1-waves from the leg motor area by transcranial magnetic stimulation. *Brain Res* 2000;859:137–46.
- [40] Ugawa Y, Rothwell JC, Day BL, Thompson PD, Marsden CD. Magnetic stimulation over the spinal enlargements. *J Neurol Neurosurg Psychiatry* 1989;52:1025–32.
- [41] Ugawa Y, Kohara N, Shimpō T, Mannen T. Magneto-electrical stimulation of central motor pathways compared with percutaneous electrical stimulation. *Eur Neurol* 1990;30:14–8.
- [42] Hamada M, Hanajima R, Terao Y, Sato F, Okano T, Yuasa K, et al. Median nerve somatosensory evoked potentials and their high-frequency oscillations in amyotrophic lateral sclerosis. *Clin Neurophysiol* 2007;118:877–86.
- [43] Arai N, Enomoto H, Okabe S, Yuasa K, Kamimura Y, Ugawa Y. Thirty minutes mobile phone use has no short-term adverse effects on central auditory pathways. *Clin Neurophysiol* 2003;114:1390–4.
- [44] Hashimoto I, Ishiyama Y, Yoshimoto T, Nemoto S. Brain-stem auditory-evoked potentials recorded directly from human brain-stem and thalamus. *Brain* 1981;104:841–59.
- [45] Kukowski B. Magnetic transcranial brain stimulation and multimodality evoked potentials in an adrenoleukodystrophy patient and members of his family. *Electroencephalogr Clin Neurophysiol* 1991;78:260–2.
- [46] Thompson PD, Day BL, Rothwell JC, Dick JP, Cowan JM, Asselman P, et al. The interpretation of electromyographic responses to electrical stimulation of the motor cortex in diseases of the upper motor neurone. *J Neurol Sci* 1987;80:91–110.

Zellweger Syndrome Caused by PEX13 Deficiency: Report of Two Novel Mutations

O.Y. Al-Dirbashi,^{1,2} R. Shaheen,² M. Al-Sayed,³ M. Al-Dosari,⁴ N. Makhseed,⁵ L. Abu Safieh,² T. Santa,⁶ B.F. Meyer,² N. Shimozaawa,⁷ and F.S. Alkuraya^{2,8,9,10*}

¹National Laboratory for Newborn Screening, King Faisal Specialist Hospital and Research Centre, Riyadh, Saudi Arabia

²Department of Genetics, King Faisal Specialist Hospital and Research Centre, Riyadh, Saudi Arabia

³Department of Medical Genetics, King Faisal Specialist Hospital and Research Centre, Riyadh, Saudi Arabia

⁴Department of Neuroscience, King Faisal Specialist Hospital and Research Centre, Riyadh, Saudi Arabia

⁵Aljahra Hospital, Kuwait City, Kuwait

⁶Graduate School of Pharmaceutical Sciences, The University of Tokyo, Tokyo, Japan

⁷Division of Genomics Research, Life Science Research Center, Gifu University, Gifu, Japan

⁸Department of Pediatrics, College of Medicine, King Saud University, Riyadh, Saudi Arabia

⁹Department of Anatomy and Cell Biology, College of Medicine, Alfaisal University, Riyadh, Saudi Arabia

¹⁰Division of Genetics and Metabolism, Department of Medicine, Children's Hospital Boston and Harvard Medical School, Boston, Massachusetts

Received 6 November 2008; Accepted 23 March 2009

Peroxisomal biogenesis disorders represent a group of genetically heterogeneous conditions that have in common failure of proper peroxisomal assembly. Clinically, they are characterized by a spectrum of dysmorphism, neurological, liver, and other organ involvement. To date, mutations in 13 PEX genes encoding peroxins have been identified in patients with peroxisomal biogenesis disorders. Mutations in *PEX13*, which encodes peroxisomal membrane protein PEX13, are among the least common causes of peroxisomal biogenesis disorders with only three mutations reported so far. Here, we report on two infants whose clinical and biochemical profile was consistent with classical Zellweger syndrome and whose complementation analysis assigned them both to group H of peroxisomal biogenesis disorders. We show that they harbor two novel mutations in *PEX13*. One patient had a genomic rearrangement resulting in a 147 kb deletion that spans the whole of *PEX13*, while the other had an out-of-frame deletion of 14 bp. This represents the first report of a *PEX13* deletion and suggests that further work is needed to examine the frequency of *PEX13* mutations among Arab patients with peroxisomal biogenesis disorders. © 2009 Wiley-Liss, Inc.

Key words: peroxisomal biogenesis disorder; *PEX13*; deletion; Zellweger syndrome

INTRODUCTION

Peroxisomes are subcellular organelles that catalyze several metabolic pathways mainly related to lipid metabolism and are found in all eukaryotic cells [Wanders, 1992]. The importance of these highly conserved organelles is evident from the severe clinical consequences

that result from defects in their structure or function. Known as peroxisomal disorders (PDs), this expansive group of congenital diseases has been divided into peroxisomal biogenesis disorders (PBDs), and disorders related to single peroxisomal enzyme deficiencies [Shimozaawa, 2007]. PBDs are autosomal recessive conditions caused by defects in either the biogenesis of peroxisomal membrane proteins encoded by PEX 16, PEX 3, and PEX 19 genes, or defects in the import of peroxisomal matrix protein, encoded by

How to Cite this Article:

Al-Dirbashi OY, Shaheen R, Al-Sayed M, Al-Dosari M, Makhseed N, Abu Safieh L, Santa T, Meyer BF, Shimozaawa N, Alkuraya FS. 2009. Zellweger syndrome caused by PEX13 deficiency: Report of two novel mutations. *Am J Med Genet Part A* 149A:1219–1223.

Additional supporting information may be found in the online version of this article.

O.Y. Al-Dirbashi's present address is Ontario Newborn Screening Laboratory, Children's Hospital of Eastern Ontario, 401 Smyth Road, Ottawa, ON, Canada K1H 8L1.

*Correspondence to:

F.S. Alkuraya, M.D., Department of Genetics, King Faisal Specialist Hospital and Research Center, MBC 03, P.O. Box 3354, Riyadh 11211, Saudi Arabia. E-mail: falkuraya@kfsrhc.edu.sa

Published online 15 May 2009 in Wiley InterScience (www.interscience.wiley.com)

DOI 10.1002/ajmg.a.32874

various other PEX genes. Functional complementation assay in fibroblasts of PBD patients revealed the existence of 13 complementation groups, each corresponding to a specific PEX gene deficiency [Shimozawa, 2007]. To date, mutations in all 13 PEX genes have been reported in patients with PBDs [Shimozawa, 2007]. Mutations in PEX13 are among the least frequently encountered with only three mutations reported worldwide in patients presenting with Zellweger syndrome, the prototype of PBDs, and the less severe phenotype of neonatal adrenoleukodystrophy [Liu et al., 1999; Shimozawa et al., 1999; Krause et al., 2006]. Recently, we have started to molecularly characterize patients with biochemically confirmed PBDs who are referred to our institution. The first two patients studied were found to belong to complementation group H caused by PEX13 deficiency. Novel deletions, one of which encompasses the entire gene, were identified in both patients.

MATERIALS AND METHODS

Patients

The two patients reported here are part of a comprehensive ongoing study of the mutation spectrum in PD patients referred to our institution. Details of the study will be described at length separately. Briefly, patients with a clinical picture consistent with PDs are enrolled if they demonstrate elevated very-long chain fatty acids (VLCFA), pristanic or phytanic acids in plasma measured by liquid chromatography tandem mass spectrometry [Al-Dirbashi et al., 2008]. Institutional Review Board approval for the study was obtained and patients were only enrolled with full informed consent. Skin biopsy and blood samples were collected from each patient for complementation and immunofluorescence and for DNA analysis, respectively.

Complementation and Microscopic Analysis

Peroxisomes in fibroblasts were visualized by indirect immunofluorescence microscopy [Shimozawa et al., 1992]. Complementation analysis was performed essentially as previously described [Yajima et al., 1992]. Briefly, patient fibroblasts were fused serially with fibroblast cell lines that are each deficient in 1 of the 13 known PEX genes. Peroxisomes are stained using antibodies to a 70 kDa peroxisomal integral membrane protein (PMP70) as a membrane marker, and catalase as a marker of matrix proteins. Complementation group is assigned based on the fusion partner that failed to restore the normal peroxisomal configuration.

Genomic DNA Isolation and PEX13 Analysis

Genomic DNA was isolated from whole blood collected in EDTA tubes using the Gentra DNA isolation kit (Qiagen, Valencia, CA) as described by the manufacturer. The four exons of PEX13 were amplified by PCR as six amplicons, which were bidirectionally, sequenced using a 3730xl DNA analyzer (ABI, Foster City, CA) and compared to the reference sequence of PEX13 (accession number NM_002618). The extent of the genomic deletion was determined by walking upstream and downstream of PEX13 using PCR of STS markers and exons of neighboring genes. An amplicon that spanned the breakpoint was eventually generated using the Expand high Fidelity system (Roche, Mannheim, Germany). Primer sequence for the four PEX13 exons and those used to determine the breakpoint of the large deletion are summarized in Table SI (supporting information Table SI may be found in the online version of this article). The PCR conditions are available on request.

RESULTS

The two patients were biochemically diagnosed with a PD based on considerably elevated hexacosanoic acid and ratios of tetracosanoic and hexacosanoic acid to docosanoic acid in plasma as determined on technical replicates using our previously described protocol [Al-Dirbashi et al., 2008] (Table I). Patient 1 was identified at the NICU where he was admitted immediately after birth with severe hypotonia. He had large anterior fontanelle and high forehead. His brain MRI showed a picture of polymicrogyria, lissencephaly, and poor myelination. Consistent with the MRI findings, his EEG revealed cortical dysfunction and seizure activity. He died at the NICU at 6 weeks of age with cardiopulmonary arrest. Patient 2 was also admitted to NICU shortly after birth because of severe hypotonia and had anteverted nostrils, a depressed nasal bridge, and a large, triangular face. His course in the NICU was complicated by recurrent apnea, seizures, and elevated liver enzymes. Renal ultrasound revealed the presence of multiple cysts. He remained in the NICU for 4 months before his transfer to the general pediatrics ward where he remains at 6 months of age with severe failure to thrive, progressive hepatic dysfunction, and global developmental delay.

Immunofluorescence microscopy studies revealed absence of the normal punctate staining pattern of catalase but positive immunofluorescence using the anti-human PMP70 antibody in fibroblasts from both Patients 1 and 2 (Fig. 1A), which indicated that both fibroblasts had the classical "ghost" appearance to their peroxisomes secondary to abnormal protein import. Subsequently, we performed complementation analysis, which confirmed that

TABLE I. Plasma Concentration (μM) of VLCFAs in the Two Patients

	Pristanic acid	Phytanic acid	C _{22:0}	C _{24:0}	C _{26:0}	C _{24:0} /C _{22:0}	C _{26:0} /C _{22:0}
Patient 1	0.27	0.74	14.7	31.8	9.1	2.16	0.618
Patient 2	0.44	5.13	14.1	34.5	9.3	2.44	0.662
Controls (n = 250) ^a	0.0–3.4	0.04–11.5	9.6–100.5	3.4–91.7	0.04–1.46	0.15–1.15	0.001–0.028

^aAl-Dirbashi et al. [2008].